DOI: 10.1002/cssc.201300414

# $Cu/MgAl_2O_4$ as Bifunctional Catalyst for Aldol Condensation of 5-Hydroxymethylfurfural and Selective Transfer Hydrogenation

Kristina Pupovac[b] and Regina Palkovits*[a, b]

Copper supported on mesoporous magnesium aluminate has been prepared as noble-metal-free solid catalyst for aldol condensation of 5-hydroxymethylfurfural with acetone, followed by hydrogenation of the aldol condensation products. The investigated mesoporous spinels possess high activity as solid-base catalysts. Magnesium aluminate exhibits superior activity compared to zinc and cobalt-based aluminates, reaching full conversion and up to 81% yield of the 1:1 aldol product. The high activity can be correlated to a higher concentration of basic surface sites on magnesium aluminate. Applying continuous regeneration, the catalysts can be recycled without loss of activity. Focusing on the subsequent hydrogenation of aldol condensation products, $Cu/MgAl_2O_4$ allows a selective hydrogenation and C–O bond cleavage, delivering 3-hydroxybutyl-5-methylfuran as the main product with up to 84% selectivity avoiding ring saturation. Analysis of the hydrogenation activity reveals that the reaction proceeds in the following order: C=C > C=O > C–O cleavage > ring hydrogenation. Comparable activity and selectivity can be also achieved utilizing 2-propanol as solvent in the transfer hydrogenation, providing the possibility for partial recycling of acetone and optimization of the hydrogen management.

## Introduction

Diminishing fossil-fuel reserves in combination with rising oil prices are the main driving forces in the development of alternative ways to fulfill the growing demand for chemicals and fuels. Anthropogenic climatic change is a severe threat to mankind and requires a significant reduction of the greenhouse gas emissions to avoid detrimental consequences for the globe. Therefore, renewable resources (e.g., biomass) have been in the center of scientific interest in recent years.[1] Biomass can be converted into high-value compounds and chemical intermediates and has a significant potential to serve as sustainable source of energy and organic carbon. The so called sleeping giant, 5-Hydroxymethylfurfural (HMF), is one of the most valuable building blocks accessible from biomass.[2] Owing to its functional groups, HMF can be transformed into valuable products through a great number of reactions, for example, oxidation, hydrogenation, aldol reaction, etherification, or esterification.[3] Aldol condensation is one of the most important C–C bond formation reactions. It has numerous applications in the synthesis of fine chemicals, plasticizers, and fragrances.[4] Industrial significance of these processes is responsible for an increasing effort to substitute conventional homogenous bases by new solid base catalysts. This can result in simplification of the process, promote the clean manufacturing, decrease corrosion of the reactor, as well as production costs. Heterogeneous catalysis enables easier separation of the products and continuous use of the catalyst. Among solid-base catalysts, alkali oxides, alumina, zeolites, and calcined hydrotalcites are promising candidates.[5]

In the field of renewable feedstocks, the development of integrated processes as well as a combination of two or more reactions in the same vessel over multifunctional solid catalysts gains increasingly in importance.[6] Dumesic et al. developed a route to convert furfural or HMF into long-chain alkanes.[7] In aqueous-phase processing, furfural or HMF firstly underwent an aldol condensation with acetone in the presence of basic Mg–Al-oxide catalysts. The condensation products were subsequently hydrogenated over a $Pd/Al_2O_3$ catalyst and finally transformed into liquid alkanes by dehydration/hydrogenation over bifunctional $Pt/SiO_2$–$Al_2O_3$ catalysts. In this process, where the aldol condensation and hydrogenation reactions played a key role, two different catalysts were needed. Therefore, in 2006 Dumesic and co-workers developed a bifunctional Pd/MgO–$ZrO_2$ catalyst for a single reactor, aqueous phase aldol condensation and hydrogenation reaction.[8] In 2010, Xu et al. prepared a new bifunctional noble-metal catalyst based on spinel-type materials.[9] The reported platinum/cobalt aluminate showed superior activity in aldol condensation of HMF with acetone, reaching up to 69% selectivity towards $C_8$ aldol products at 96% conversion. Additionally, this $Pd/Co_2Al_2O_4$ catalyst exhibited high activity in a subsequent hydrogenation, delivering the fully hydrogenated product 4-(2-tetrahydrofuryl)-2-butanol, with up to 75% selectivity. The study empha-

[a] Prof. Dr. R. Palkovits
Institut für Technische und Makromolekulare Chemie
RWTH Aachen University
Worringerweg 1, 52074 Aachen (Germany)
E-mail: palkovits@itmc.rwth-aachen.de

[b] K. Pupovac, Prof. Dr. R. Palkovits
Max-Planck-Institut für Kohlenforschung
Kaiser-Wilhelm-Platz 1, 45470 Mülheim an der Ruhr (Germany)

Supporting Information for this article is available on the WWW under http://dx.doi.org/10.1002/cssc.201300414.

 © 2013 Wiley-VCH Verlag GmbH & Co. KGaA, Weinheim 

sized a rapid hydrogenation of C=C and C=O bonds, while ring hydrogenation was the rate-determining step.

However, the need for solid bases with sufficient activity, selectivity, and stability to achieve an efficient aldol condensation of HMF with acetone remains. Suitable noble-metal-free catalysts for the hydrogenation of these aldol condensation products have not been investigated yet. Considering an efficient hydrogen management, the selective preparation of furan derivatives could make potential biofuels, such as 2-butenyl-5-methylfuran, accessible.

Spinel-type oxides are promising candidates because of their high thermal stability, hydrophobicity, outstanding mechanical robustness, and low surface acidity.[10] They exhibit strong resistance to acids and bases, and some aluminate spinels tend to prevent sintering of noble metals owing to strong metal–support interactions.[11,12] Spinels are prepared by calcination of suitable precursors at high temperatures, which are necessary to achieve sufficient crystallinity of these materials.[13] On the other hand, high temperature may result in materials of low specific surface area, limiting their applicability in catalysis. Promising alternative methods to synthesize spinels with high specific surface areas are co-precipitation and hydrothermal or sol–gel synthesis,[14] but it is challenging to prevent the contamination of the products by cations of the precipitate or organic residues of the precursor.

Herein, various mesoporous spinel aluminates with high specific surface area were synthesized by a facile hard-templating route based on activated carbon.[15] Obtained spinels were tested in aldol condensation of HMF with acetone, reaching 92% selectivity of HMF based aldol condensation products at full conversion. The relationships between the activity of materials and their selectivity for the desired condensation product as well as the properties of the materials could be studied to identify factors that govern aldol condensation and to establish the basis for structure–activity relationships. Aiming for the design of a multifunctional catalyst, copper was introduced into the mesoporous spinel. The obtained bifunctional noble-metal-free catalyst showed high activity and selectivity in the aldol condensation of HMF and acetone as well as in the subsequent hydrogenation of the condensation products (Scheme 1). To the best of our knowledge, this is the first example of a noble-metal-free catalyst for the selective hydrogenation of such aldol condensation products. Our study highlights the high catalytic activity and selectivity of the supported copper catalyst in transfer hydrogenation, eliminating the need for external hydrogen sources.

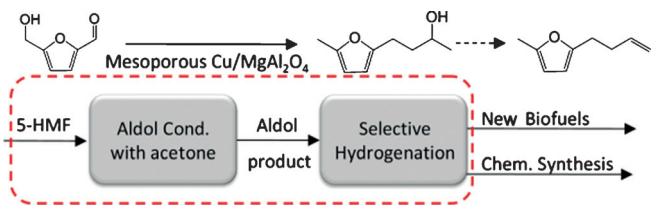


**Scheme 1.** Reaction steps catalyzed by $Cu/MgAl_2O_4$, including aldol condensation of HMF with acetone and subsequent hydrogenation.

## Results and Discussion

### Physicochemical properties of the materials

Typical TEM images of the pure spinels as well as copper supported on magnesium aluminate are shown in Figure 1. From the morphologies it is clearly visible that highly crystalline, nanometer-sized ternary oxides were obtained. The supported copper catalyst displayed well-dispersed metal nanoparticles on the spinel support (Figure 1 d).

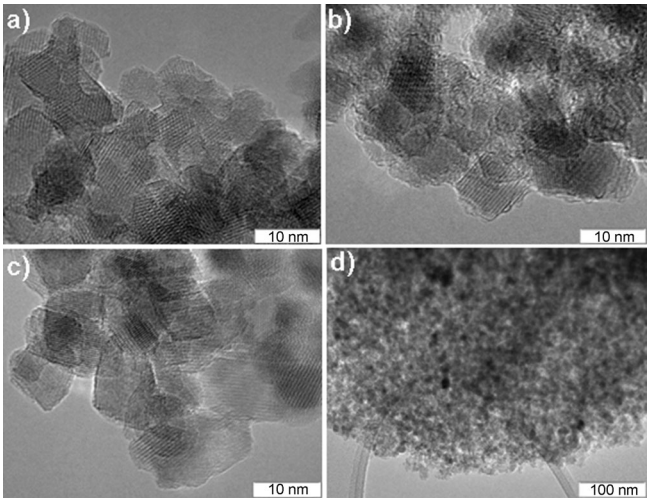


**Figure 1.** TEM images of a) $MgAl_2O_4$, b) $ZnAl_2O_4$, c) $CoAl_2O_4$, and d) $Cu/MgAl_2O_4$.

X-ray diffraction (XRD) patterns of the materials exhibit defined Bragg reflections characteristic for the spinel-phase formation (Figure 2), and the narrow reflections show successful formation of highly crystalline oxides.

Particle sizes calculated based on the line broadening of the XRD reflections by using the Scherrer equation reveal crystallites with 6 nm in diameter for $MgAl_2O_4$, 8 nm for $CoAl_2O_4$, and 16 nm for $ZnAl_2O_4$.

After impregnation of copper(II) nitrate solution on the mesoporous $MgAl_2O_4$ and subsequent reduction at 523 K for 3 h, new signals appeared, which can be assigned to pure copper, indicating that copper could be successfully introduced into the mesoporous spinel. No evidence of $CuAl_2O_4$ formation was detected. Elemental analysis confirmed a copper loading of the catalyst of 4.7 wt%, which is in good agreement with the utilized copper concentration. Concerning the copper particle size, TEM analysis revealed homogeneously distributed copper nanoparticles of around 15 nm in diameter, which are partially present as agglomerates of 40 nm size.

To further characterize the mesoporous structure of the materials, nitrogen physisorption measurements were performed. The nitrogen sorption isotherms of $ZnAl_2O_4$, $CoAl_2O_4$, $MgAl_2O_4$, and $Cu/MgAl_2O_4$, are presented in Figure 3. The isotherms have typical type-IV shape (IUPAC classification) with a nitrogen uptake at low relative pressures and a closed and well-defined hysteresis loop around a relative pressure of 0.6–0.8 $P/P_0$, char-

© 2013 Wiley-VCH Verlag GmbH & Co. KGaA, Weinheim

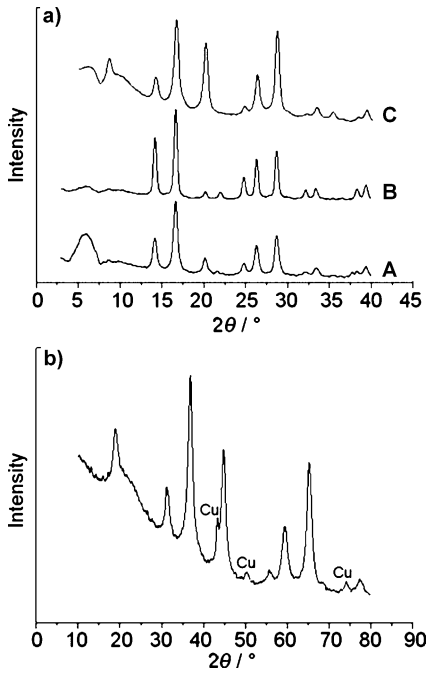


**Figure 2.** Powder XRD patterns of a) $CoAl_2O_4$ (A), $ZnAl_2O_4$ (B), $MgAl_2O_4$ (C) and b) $Cu/MgAl_2O_4$.

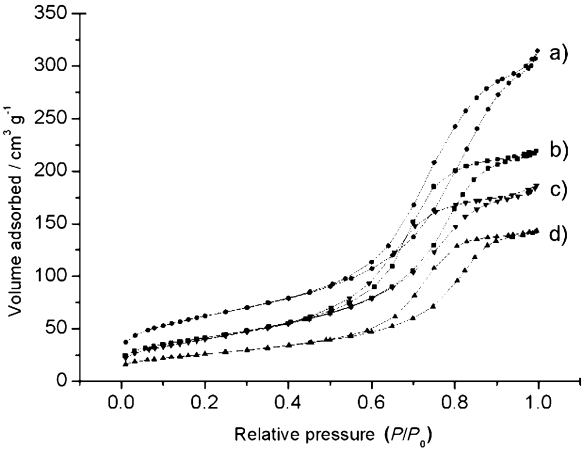


**Figure 3.** $N_2$ adsorption–desorption isotherms of a) $CoAl_2O_4$, b) $MgAl_2O_4$, c) $Cu/MgAl_2O_4$, and d) $ZnAl_2O_4$.

acteristic for materials with micro- and mesoporosity.[16] The Brunauer–Emmett–Teller (BET) surface areas of $MgAl_2O_4$, $CoAl_2O_4$, and $ZnAl_2O_4$ are 149, 224, and 96 $m^2 g^{-1}$, respectively. The materials possess a broad pore size distribution with average mesopore diameters of 9, 8.2, and 9.4 nm together with 0.34, 0.46, and 0.22 $cm^3 g^{-1}$ pore volume for $MgAl_2O_4$, $CoAl_2O_4$, and $ZnAl_2O_4$, respectively. Additional impregnation of copper on magnesium aluminate resulted in a spinel material with 147 $m^2 g^{-1}$ specific surface area, 0.29 $cm^3 g^{-1}$ total pore volume, and an average mesopore diameter of 7.8 nm. This indicates that the metal has no significant influence on the porosity and specific surface area of the material. Considering XRD analysis and nitrogen sorption experiments, the porosity of the obtained spinels can be mainly assigned to interparticle porosity caused by template-assisted material synthesis.

### Aldol condensation of HMF

The catalytic activity of high surface area spinel oxides was tested in the aldol condensation of HMF with acetone, for which acetone was used as a substrate and as a solvent. Because of the acetone excess, the main and desired product was (*E*)-4-[5-(hydroxymethyl)furan-2-yl]but-3-en-2-one (**1**) (Scheme 2a). Owing to the symmetry of acetone molecules, further condensation with HMF was possible, leading to the formation of (1*E*,4*E*)-1,5-bis[5-(hydroxymethyl)furan-2-yl]penta-1,4-dien-3-one (**2**) as the minor product.

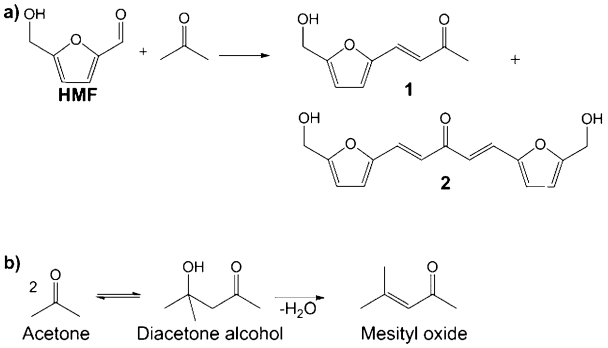


**Scheme 2.** Reaction pathway of a) aldol condensation of HMF with acetone and b) self-condensation of acetone.

The aldol condensation of HMF with acetone, presented in Scheme 2a, occurs on basic sites in the first step by initial abstraction of the α-proton from acetone, leading to the formation of a carbanion species. In the second step, the formation of a β-hydroxyl ketone takes place. Finally, by elimination of one water molecule from the unstable intermediate, the α,β-unsaturated ketone **1** is formed. In parallel, self-condensation of acetone as a side reaction can occur, leading to the formation of diacetone alcohol, which readily dehydrates to mesityl oxide (MO; Scheme 2b).

The reaction rate of the aldol condensation between HMF and acetone only depends on HMF concentration, as acetone is used as both, the substrate and the solvent. Thus, acetone is available in excess and its concentration change during reaction can be neglected. The kinetic analysis emphasizes a first-order behavior (Figure 4).

The results obtained in the aldol condensation of HMF with acetone at optimum reaction conditions are summarized in Table 1. The complete conversion of HMF was obtained after 7 h of reaction time. When magnesium aluminate was used as a catalyst, the maximum total yield of aldol products **1** and **2** reached 92%. A high selectivity towards **1** of 81% was observed, and in all cases the formation of product **2** was around 10%. The competitive self-condensation reaction of acetone and subsequent dehydration to MO took place to a very limited extent (below 1% yield).[17]

© 2013 Wiley-VCH Verlag GmbH & Co. KGaA, Weinheim

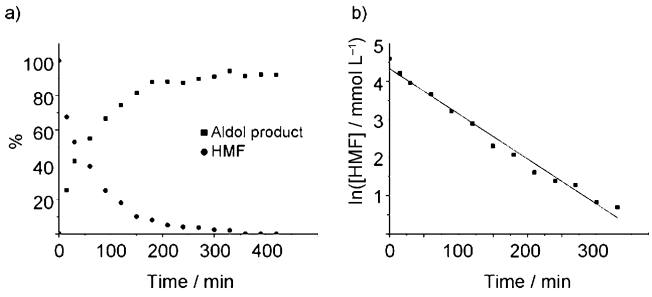


**Figure 4.** Kinetic analysis of aldol condensation between HMF and acetone: a) reaction profile and b) plot of logarithms of HMF concentration versus time for HMF disappearance [373 K, $MgAl_2O_4$, HMF/catalyst = 1.5 (*w*/*w*)].

**Table 1.** Catalytic performance of the synthesized spinels in the aldol condensation of HMF and acetone at optimized reaction conditions [413 K; 7 h, HMF/catalyst = 2 (*w*/*w*)].

| Catalyst | Selectivity [%] | | HMF conversion |
|---|---|---|---|
| | **1** | **2** | [%] |
| $MgAl_2O_4$ | 81 | 11 | 100 |
| $CoAl_2O_4$ | 70 | 10 | 100 |
| $ZnAl_2O_4$ | 76 | 10 | 100 |
| $Cu/MgAl_2O_4$ | 78 | 7 | 100 |

To estimate the maximum possible formation of MO, self-condensation of acetone was performed in the presence of $MgAl_2O_4$ as a catalyst; a maximum yield of 5%MO was reached. The suppression of MO formation in the presence of HMF demonstrates a preferential reaction between HMF and acetone. Therefore, the consideration of MO has been omitted in the further study, owing to its negligible formation. The main side product in the process can be assigned to the products derived from HMF oligomerization.

To estimate the catalytic activity of the investigated materials, the aldol reaction was stopped after 30 min to ensure that the reaction was not completed, as a fair comparison of catalysts is not possible at full conversion. Corresponding data are listed in Table 2. The conversion over $ZnAl_2O_4$ and $CoAl_2O_4$ is considerably lower compared to $MgAl_2O_4$ as the initial rate increased from 2.10 mol min$^{-1}$ g$^{-1}$ for $ZnAl_2O_4$ to 7.38 mol min$^{-1}$ g$^{-1}$ for $MgAl_2O_4$. In the latter case, the conversion reaches 60% with a selectivity of product **1** as high as 89%. Accordingly, the results presented in Table 2 indicate that the order of activity is Mg > Co > Zn. Considering the specific surface area of the different spinels, the superior activity of $MgAl_2O_4$ was confirmed. With regard to $ZnAl_2O_4$ and $CoAl_2O_4$, both materials reached a comparable surface-related reaction rate of 2.19 and $1.88 \times 10^{-6}$ mol min$^{-1}$ m$^{-2}$, respectively. Variation of the catalyst concentration at constant reaction conditions demonstrates an almost linear increase up to a conversion of approximately 90%, emphasizing that the obtained data are in the kinetic region (Figure 5). Interestingly, $CoAl_2O_4$ and $ZnAl_2O_4$ showed

**Table 2.** Initial reaction rates (normalized to the weight and the specific surface area of the material) obtained for different catalysts after 30 min reaction time [413 K, HMF/catalyst = 4.5 (*w*/*w*)].

| Catalyst | Reaction rate | | HMF conv. | Select. to |
|---|---|---|---|---|
| | [$10^{-4}$ mol min$^{-1}$ g$^{-1}$] | [$10^{-6}$ mol min$^{-1}$ m$^{-2}$] | [%] | **1** [%] |
| $MgAl_2O_4$ | 7.38 | 4.95 | 60 | 89 |
| $CoAl_2O_4$ | 4.21 | 1.88 | 47 | 77 |
| $ZnAl_2O_4$ | 2.10 | 2.19 | 19 | 85 |

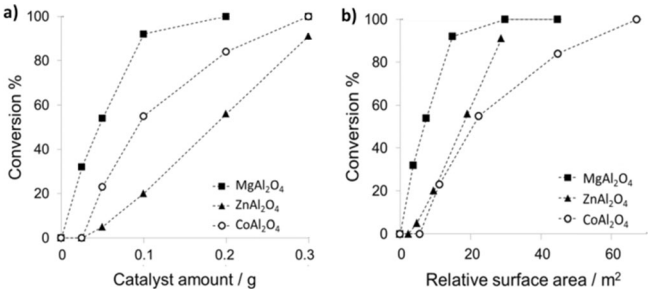


**Figure 5.** Effect of the amount of catalyst on HMF conversion (480 mg HMF, 413 K, 5 h).

a delayed activity increase, which was reproduced and could be related to an induction period or to a high experimental error at low conversions. Further studies will focus on this effect. From these observations, we conclude that the conversion increases because of the linear increase of available basic sites on the surface of spinel catalysts. The relative differences between the activities of $MgAl_2O_4$, $ZnAl_2O_4$,and $CoAl_2O_4$, can be related to the concentration and the strength of basic sites on these materials. Considering the above discussed results, it is possible to establish the following order of basicity: Mg > Co ≈ Zn. To further investigate the basic properties of the solid catalysts, temperature-programmed desorption (TPD) using $CO_2$ as a probe molecule was conducted. The $CO_2$-TPD results presented in Figure 6 suggest that several binding sites are available on the nonuniform surface of the spinels.

All spinel materials show complex desorption profiles, which are owed to the presence of a variety of basic sites of different strength.[18] The desorption peaks in the low-temperature range (up to 450 K) can be attributed to $CO_2$ interacting with Brønsted hydroxyl groups on the spinel surface forming bicarbonate species that are related to basic sites of low strength. The desorption peaks in the medium temperature range (450–650 K) can be attributed to the bidentate carbonate species. They form acid–base pairs such as $M^{2+}$–$O^{2-}$ or $M^{3+}$–$O^{2-}$ and can be related to basic sites of medium strength. The desorption peaks at high temperatures (from 700 K) result from unidentate carbonates released from low-coordination oxygen anions and are related to basic sites of high strength. Interestingly, compared to zinc and cobalt aluminates, bicarbonate was the predominant species formed on $MgAl_2O_4$, indicating that Brønsted hydroxyl groups could be the active basic sites responsible for the superior catalytic activity of $MgAl_2O_4$. Intensities of the TPD spectra indicate that the total amount of $CO_2$ desorbed on $MgAl_2O_4$ is much higher when compared to zinc and cobalt alu-

© 2013 Wiley-VCH Verlag GmbH & Co. KGaA, Weinheim

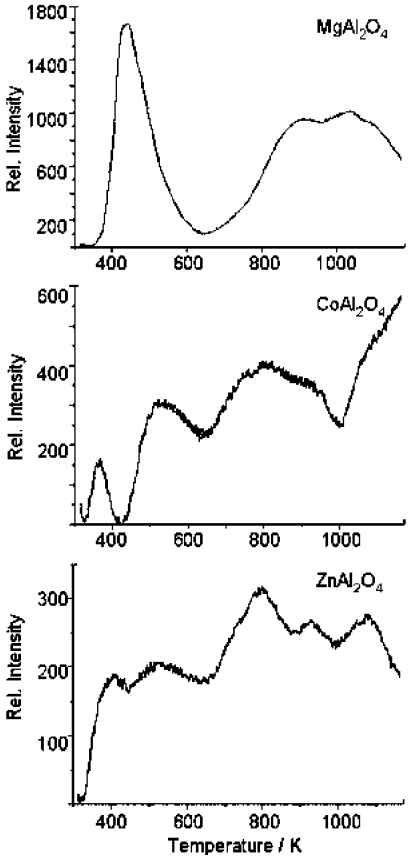


**Figure 6.** $CO_2$–TPD spectra of a) $MgAl_2O_4$, b) $CoAl_2O_4$, and c) $ZnAl_2O_4$.

minate although its specific surface area is only two thirds of $CoAl_2O_4$. These measurements indicate that $MgAl_2O_4$ has predominantly weak basic sites, but possesses a significantly higher surface concentration of basic sites compared to the other two spinels. As only little differences in selectivity of the catalysts were detected, the overall concentration of basic sites appears to be decisive to achieve high yields of the desired aldol condensation product.

Reusability and regeneration of a solid-base catalyst is of considerable importance; therefore, experiments to study the recyclability of spinel catalysts were conducted. After reaction, spent $MgAl_2O_4$ was filtered off, washed with acetone, dried, and used in the next aldol reaction. Deactivation of the catalyst, as well as a color change from white to dark orange, was observed. Catalyst deactivation may be caused by adsorption of reaction products that block active sites on the catalyst surface. Accordingly, thermogravimetric analysis confirms a weight loss of the catalyst after reaction at around 623 K (Supporting Information, Figure S1). Applying a calcination step after reaction, the catalyst can be recycled up to four cycles without any significant loss in activity (Figure 7).

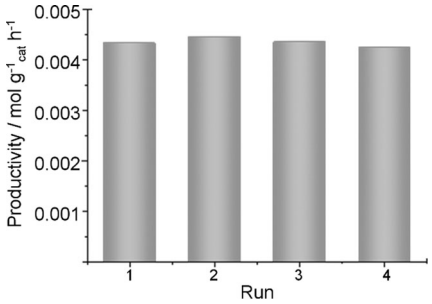


**Figure 7.** Reusability of the $MgAl_2O_4$ catalyst at 373 K.

### Hydrogenation of aldol condensation products over bifunctional catalysts

To design a multifunctional catalyst, metal was introduced into a mesoporous spinel. The bifunctional noble-metal-free catalyst $Cu/MgAl_2O_4$ was tested in the aldol condensation reaction, and its performance was compared to pure $MgAl_2O_4$. As presented in Table 1, the bifunctional catalyst reached an activity comparable to pure $MgAl_2O_4$, indicating that the metal loading has no influence on the basic properties of the catalyst. Following aldol condensation, the residual acetone was removed by rotary evaporation and the subsequent hydrogenation reaction over the same $Cu/MgAl_2O_4$ catalyst was continued by adding 10 mL of 2-propanol and pressurizing the system to 50 bar $H_2$. Several possible hydrogenation products highlighting the challenge associated with the development of selective catalysts for this application are presented in Scheme 3.

Previous studies focused on fully hydrogenated products (**4**) and the formation of alkanes based on aldol products of HMF.[7–9,19] However, the main challenge concerns a selective reduction of the oxygen content of renewable feedstocks with minimum hydrogen demand.

The hydrogenation reaction of **1** over $Cu/MgAl_2O_4$ catalyst proceeds through parallel and consecutive reaction pathways that involve hydrogenation of C=O and C=C bonds. The reaction was studied to gain deeper insights into the hydrogenation of the different functional groups.

First, the C=C double bond of the substrate was hydrogenated, forming **2**. With prolonged reaction time the reduction of the carbonyl group of **3** as well as the deoxygenation of the C–O bond took place, which resulted in the formation of **6**. After 7 h of reaction, the aldol product **1** was completely consumed delivering **6** with a selectivity of up to 82%. Time variation at constant temperature and temperature variation emphasize the described reaction sequence (Figure 8). At 373 K **3** was found to be the main product with 69% selectivity. A further increase of the reaction temperature initialized C–O bond cleavage, delivering the deoxygenated product **6** as the main product at a reaction temperature of 513 K. Moreover, small amounts of dimeric aldol products (Scheme 2) were successfully transformed into the deoxygenated form (Supporting Information, Figure S2).

### Copper-based hydrogenation catalysts and transfer hydrogenation

For all temperature ranges, $Cu/MgAl_2O_4$ results in a preferential deoxygenation of the C–O bond of the primary alcohol com-

© 2013 Wiley-VCH Verlag GmbH & Co. KGaA, Weinheim

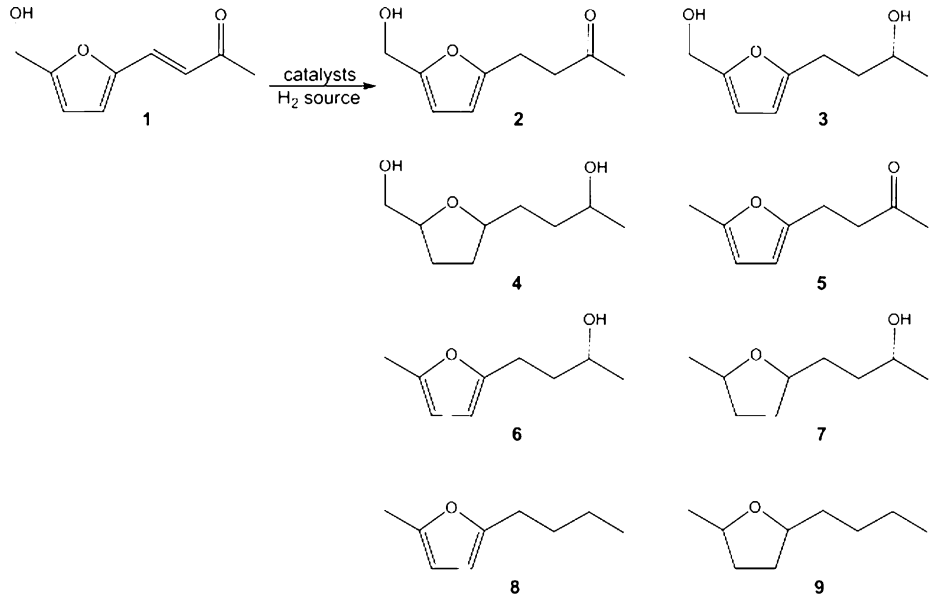


**Scheme 3.** Possible hydrogenation products derived from **1**.

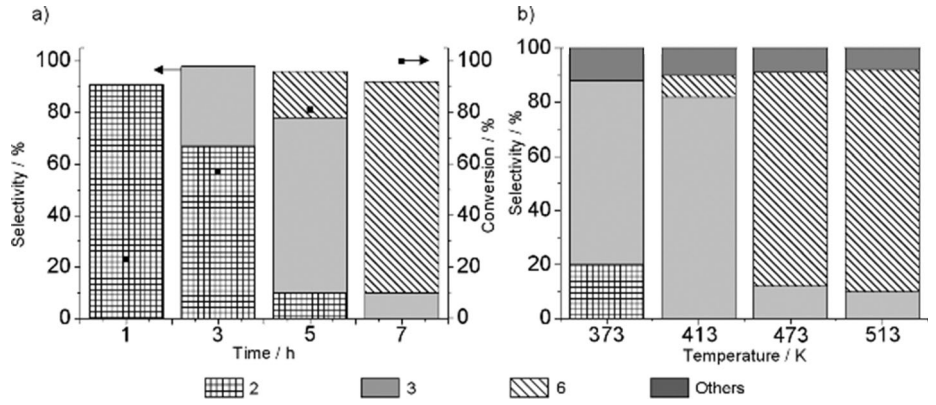


**Figure 8.** Hydrogenation of aldol product **1** over $Cu/MgAl_2O_4$ a) at 473 K at different time intervals and b) at different temperatures for 7 h reaction time allowing full conversion.

pared to the hydrogenation of the aromatic ring. This selectivity is typical for copper catalysts, which are known for their high efficiency toward C–O hydro-deoxygenation.[20] Commercially available copper-based catalysts such as copper chromite, $CuO/ZnO/Al_2O_3$, Raney copper, and copper oxides, were investigated in the hydrogenation reaction (Table 3). All materials allowed complete conversion of **1**, but demonstrated different product distributions. For example, copper chromite, which is known for hydrogenolysis and decarboxylation reactions,[21] delivered **6** as the main product. The catalyst utilized in industrial methanol synthesis, $CuO/ZnO/Al_2O_3$, was active, reaching up to 80% yield of **6**.[22] In contrast, copper oxide showed poor selectivity towards the formation of **6**, but enabled a partial hydrogenation to products **3** and **5**. We assume that under operating conditions the reduction of $Cu^I$ and $Cu^{II}$ to $Cu^0$ occurs, but that it might be influenced by the catalyst composition as well as the catalyst support.[20] Experiments with Raney copper and $Cu/MgAl_2O_4$ fully reduced to $Cu^0$ before reaction allowed an efficient transformation of **1** to **6**, further emphasizing the role of $Cu^0$ in the reaction. Further studies are certainly needed to clarify the active species under reaction conditions as well as the impact of copper surface area and support materials on activity and selectivity in the hydrogenation of HMF aldol products. Unfortunately, a selective C–O cleavage of both the primary and the secondary alcohol without hydrogenation of the aromatic ring or ring-opening hydrogenation has not been achieved yet. These products will be the focus of future studies and would certainly present a highly interesting product for application as high-boiling solvents and new biofuel compounds.

**Table 3.** Hydrogenation of aldol product **1** over different commercial catalysts and $Cu/MgAl_2O_4$.

| Catalyst | HMF conv. [%] | Select. to **6** [%] |
|---|---|---|
| copper chromite | 100 | 77 |
| $CuO/ZnO/Al_2O_3$ | 100 | 80 |
| Raney copper | 100 | 82 |
| $Cu_2O$ | 100 | – |
| CuO | 100 | 16 |
| $Cu/MgAl_2O_4$ | 100 | 84 |

Performing the hydrogenation reaction of **1** at 473 K for 7 h and at 50 bar $H_2$ pressure, the recycling of the noble-metal-free $Cu/MgAl_2O_4$ catalyst was investigated. After the first reaction run, the catalyst was filtered off, washed, dried, and used for a subsequent hydrogenation cycle. As depicted in Figure 9, the fresh catalyst reached complete conversion of **1** with 80% selectivity to the desired product **6**. In the following recycling runs, the conversion of **1** remained unchanged whereas the selectivity towards **6** decreased. According to the XRD measurement, the structure of the copper-supported spinel remained intact after four consecutive runs. However, elemental analysis shows that the copper loading decreased from 4.7 to 3.8 wt%, which consequently influenced the final selectivity of the catalyst. Filtration experiments emphasized that soluble copper species only contributed to a minor fraction of the observed

© 2013 Wiley-VCH Verlag GmbH & Co. KGaA, Weinheim

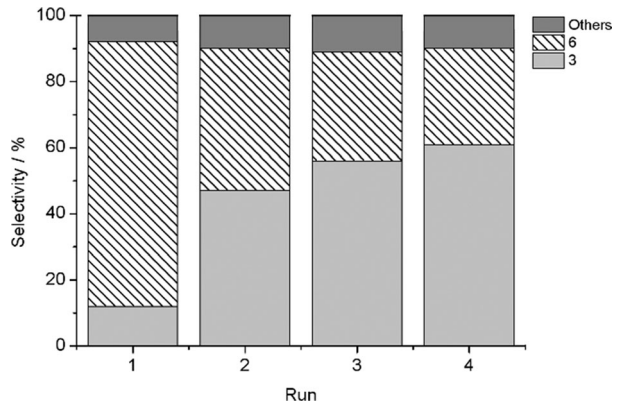


**Figure 9.** Recycling of $Cu/MgAl_2O_4$ in hydrogenation reaction of **1**.

catalytic activity. The TEM analysis emphasized significant sintering of the copper particles to above 50 nm (Supporting Information, Figures S3–S5); therefore, further optimization of the catalyst to enhance its stability and recyclability will be the focus of future investigations.

One challenge of hydrogenation reactions is the demand of high hydrogen pressures. Using secondary alcohols as reaction solvent provides an opportunity to investigate transfer hydrogenation. Using 2-propanol as a source of hydrogen and $Cu/MgAl_2O_4$ as a catalyst, the hydrogenation reaction was performed in a 36 mL stainless steel reactor over night at 518 K. During the reaction, the solvent was in a supercritical state ($T_{cr}=508$ K, $p_{cr}=47.6$ bar for 2-propanol), resulting in a pressure of up to 70 bar. The transfer hydrogenation delivered also **6** as final product with up to 77% selectivity, which is in good agreement with the results obtained previously using hydrogen pressure. Overall, a process integration combining aldol condensation with acetone and transfer hydrogenation delivering acetone becomes possible. Future studies will focus on further reaction integration to avoid intermediate separation steps.

## Conclusions

Our investigations demonstrate that highly crystalline, mesoporous spinels are efficient catalysts for the aldol condensation of HMF with acetone. Among the investigated materials, $MgAl_2O_4$ reached the highest activity with up to 81% of the HMF–acetone 1:1 product. The higher activity of $MgAl_2O_4$ compared to $ZnAl_2O_4$ and $CoAl_2O_4$ can be assigned to the higher density of available Brønsted basic sites (OH-groups) on the surface of the catalyst. The regeneration and recyclability tests confirmed that $MgAl_2O_4$ can be reused after regeneration without any significant loss in activity. Moreover, a new bifunctional noble-metal-free $Cu/MgAl_2O_4$ catalyst was highly efficient in the aldol condensation indicating that copper has no influence on structure, porosity, and basic properties of $MgAl_2O_4$. The $Cu/MgAl_2O_4$ catalyst was used in the hydrogenation of condensation products and showed high selectivity for C–O bond cleavage of primary alcohols, delivering 3-hydroxybutyl-5-methylfuran (**6**) as the main product. The bifunctional catalyst was successfully tested in the transfer hydrogenation using 2-propanol as hydrogen source and also delivered **6** as the main product in selectivities of up to 77%.

## Experimental Section

### Catalyst preparation

The pure oxide spinels were prepared through the activated carbon route.[15] Activated carbon was purchased from Rütgers/CarboTech (BET surface area of 1650 $m^2g^{-1}$ and pore volume of 0.79 $cm^3g^{-1}$) and used as received. In a typical synthesis, a mixture of concentrated metal nitrate solution with the ratio of $M^{3+}/M^{2+}=2:1$ was added to carbon (10 g). Impregnation was performed under vigorous stirring for 20 min. The impregnated carbon was directly placed in a porcelain dish in a box oven and heated to the calcination temperature (823 K for $ZnAl_2O_4$ and $CoAl_2O_4$; 1023 K for $MgAl_2O_4$) for 4 h with a heating rate of 4 $Kmin^{-1}$. The bifunctional $Cu/MgAl_2O_4$ catalyst was prepared by impregnating the copper nitrate solution (5 wt% Cu) on the freshly synthesized $MgAl_2O_4$ spinel. The following reduction of the metal supported catalyst was performed in a tube oven with $H_2$ at 523 K for 3 h (5 $Kmin^{-1}$ heating rate).

### Catalyst characterization

The nitrogen sorption isotherms were measured at 77 K by using an ASAP 2010 sorption analyzer (Micromeritics). The samples were outgassed in vacuum at 473 K for 6 h prior to measurements. The powder XRD patterns of $CoAl_2O_4$, $ZnAl_2O_4$, and $MgAl_2O_4$ were recorded on a Stoe STADI P transmission diffractometer ($MoK_{\alpha1}$: 0.7093 Å) and the XRD pattern of $Cu/MgAl_2O_4$ was recorded on a Stoe STADI P transmission diffractometer ($CuK_{\alpha1}$: 1.54016 Å), both equipped with a primary Ge (111) monochromator and a linear position sensitive detector. The samples were filled into glass capillaries with 0.5 mm in diameter, and data collection was performed at room temperature. TEM images were recorded by using a 200 kV cold field emitter Hitachi HF 2000 equipped with Si(Li) EDX detector. The thermogravimetric analysis (TGA) of the spinel sample was performed by using a Netzsch STA 449 C thermobalance under argon with a heating rate of 10 $Kmin^{-1}$. The temperature-programmed desorption of $CO_2$ was studied by using a Thermo Electron Corporation TPDRO 1100 series catalytic Surfaces Analyzer equipped with a thermocouple (TC) detector. Prior to the adsorption of the probe molecule, the sample (approximately 135 mg) was cleaned by a helium stream for 1 h. After that, the desorption process was performed from 423 to 1173 K at 10 $Kmin^{-1}$ under helium flow.

### Aldol condensation/Hydrogenation and product analysis

A typical aldol condensation of HMF with acetone was performed for 5 h at 373–413 K with a substrate to catalyst ratio of 4.5 with a HMF concentration of 0.045 $gmL^{-1}$, if not specified differently. After the reaction, residual acetone was removed by rotary evaporation and the hydrogenation was continued by adding 10 mL 2-propanol and catalyst (except when bifunctional noble-metal-free $Cu/MgAl_2O_4$ was used as catalyst). The system was pressurized with 50 bar $H_2$ and the hydrogenation was performed at elevated temperatures for 7 h. The quantification of HMF and aldol condensation products was performed by using a HPLC (Agilent 1260 Infinity) equipped with a 50 mm Zorbax Eclipse Puls C18 column

© 2013 Wiley-VCH Verlag GmbH & Co. KGaA, Weinheim

(4.6 mm inner diameter) and UV detector (250 nm). The methanol/water gradient was used as eluent (A: 30% methanol; B: 90% methanol; linear gradient from 100% A to 100% B in 5 min.). The hydrogenation products were analyzed by using an AT 6890 N gas chromatograph (Agilent) equipped with a 30 m DB–1 column and a flame ionization detector (FID). The quantification of the hydrogenation products was based on the internal standard method and the area normalization method.

## Acknowledgements

*We thank Dr. C. Weidenthaler for XRD analyses, B. Spliethoff for TEM analyses and valuable discussions, and A. Deege and H. Hinrichs for HPLC analysis. This work was funded by the European Research Council (Grant No. 247081) and the Cluster of Excellence "Tailor-Made Fuels from Biomass" funded by the Excellence Initiative by the German federal and state governments to promote science and research at German universities.*

**Keywords:** 5-hydroxymethylfurfural · aldol reaction · copper · heterogeneous catalysis · hydrogenation

[1] V. I. Sharkov, *Angew. Chem. Int. Ed. Engl.* **1963**, *2*, 405 – 409; D. Brownlie, *J. Soc. Chem. Ind.* **1940**, *59*, 671 – 675.
[2] a) A. Corma, S. Iborra, A. Velty, *Chem. Rev.* **2007**, *107*, 2411 – 2502; b) R.-J. van Putten, J. C. van der Waal, E. de Jong, C. B. Rasrendra, H. J. Heeres, J. G. de Vries, *Chem. Rev.* **2013**, *113*, 1499 – 1597.
[3] R. M. Musau, R. M. Munavu, *Biomass* **1987**, *13*, 67 – 74; T. Ståhlberg, E. Eyjolfsdottir, Y. Y. Gorbanev, I. Sadaba, A. Riisager, *Catal. Lett.* **2012**, *142*, 1089 – 1097.
[4] J. March, *Advanced Organic Chemistry, 4th ed.*, Wiley, New York, **1992**, p. 938; A. Ueda, Y. Fujita, H. Emoto, A. Adachi (Mitsubishi Chem. Corp.), European Patent 99-123711, **2000**; J. C. A. A. Roelofs, A. J. van Dillen, K. P. de Jong, *Catal. Lett.* **2001**, *74*, 91 – 94; K. Bauer, D. Garbe, H. Surburg, *Common Fragrance and Flavor Materials, 2nd ed.*, Wiley-VCH, Weinheim, **1990**.
[5] M. J. Climent, A. Corma, S. Iborra, A. Velty, *Catal. Lett.* **2002**, *79*, 157 – 163; A. Corma, R. M. Martin-Aranda, *J. Catal.* **1991**, *130*, 130 – 137; C. Noda, G. P. Alt, R. M. Werneck, C. A. Henriques, J. L. F. Monteiro, *Braz. J. Chem. Eng.* **1998**, *15*, 120 – 125.
[6] J. I. Di Cosimo, G. Torres, C. R. Apesteguia, *J. Catal.* **2002**, *208*, 114 – 123.
[7] G. W. Huber, J. N. Chheda, C. J. Barrett, J. A. Dumesic, *Science* **2005**, *308*, 1446 – 1450.
[8] C. J. Barrett, J. N. Chheda, G. W. Huber, J. A. Dumesic, *Appl. Catal. B* **2006**, *66*, 111 – 118.
[9] W. Xu, X. Liu, J. Ren, P. Zhang, Y. Wang, Y. Guo, Y. Guo, G. Lu, *Catal. Commun.* **2010**, *11*, 721 – 726.
[10] S. Farhadi, S. Panahandehjoo, *Appl. Catal. A* **2010**, *382*, 293 – 302; G. L. Fan, J. Wang, F. Li, *Catal. Commun.* **2011**, *15*, 113 – 117.
[11] G. Aguilar-Ros, M. A. Valenzuela, H. Armendariz, P. Salas, J. M. Dominguez, D. R. Acosta, I. Schifter, *Appl. Catal A: Gen.* **1992**, *90*, 25 – 34.
[12] H. Matsui, C. Xu, H. Tateyama, *Appl. Phys. Lett.* **2001**, *78*, 1068 – 1070; M. A. Valenzuela, P. Bosch, G. Aguilar-Rios, B. Zapata, C. Maldonado, I. Schifter, *J. Mol. Catal.* **1993**, *84*, 177 – 186.
[13] K. Sampath, F. Cordaro, *J. Am. Ceram. Soc.* **1998**, *81*, 649 – 654.
[14] G. Aguilar-Ríos, M. Valenzuela, P. Salas, H. Armendariz, P. Bosch, G. Del Toro, R. Silva, V. Bertin, S. Castillo, A. Ramirez-Solis, I. Schifter, *Appl. Catal. A* **1995**, *127*, 65 – 75; M. Zawadzki, J. Wrzyszcz, *Mater. Res. Bull.* **2000**, *35*, 109 – 114; A. R. Phani, M. Passacantando, S. Santucci, *Mater. Chem. Phys.* **2001**, *68*, 66 – 71.
[15] M. Schwickardi, T. Johann, W. Schmidt, F. Schüth, *Chem. Mater.* **2002**, *14*, 3913 – 3919.
[16] I. Langmuir, *J. Am. Chem. Soc.* **1918**, *40*, 1361 – 1403.
[17] S. Lippert, W. Baumann, K. Thomke, *J. Mol. Catal.* **1991**, *69*, 199 – 214; G. G. Podrebarac, F T. T. Ng, G. L. Rempel, *Chem. Eng. Sci.* **1997**, *52*, 2991 – 3002.
[18] J. I. Di Cosimo, V. K. Diez, M. Xu, E. Inglesia, C. R. Apesteguia, *J. Catal.* **1998**, *178*, 499 – 510; M. Bolognini, F. Cavani, D. Scagliarini, C. Flego, C. Perego, M. Saba, *Catal. Today* **2002**, *75*, 103 – 111; V. K. Díez, C. R. Apesteguia, J. I. Di Cosimo, *J. Catal.* **2003**, *215*, 220 – 233.
[19] J. Julis, M. Hölscher, W. Leitner, *Green Chem.* **2010**, *12*, 1634 – 1639; J. Julis, W. Leitner, *Angew. Chem.* **2012**, *124*, 8743 – 8747; *Angew. Chem. Int. Ed.* **2012**, *51*, 8615 – 8619.
[20] K. Tajvidi, K. Pupovac, M. Kükrek, R. Palkovits, *ChemSusChem* **2012**, *5*, 2139 – 2142.
[21] K. L. Deutsch, B. H. Shanks, *J. Catal.* **2012**, *285*, 235 – 241.
[22] C. Baltes, S. Vukojevic, F. Schüth, *J. Catal.* **2008**, *258*, 334 – 344.

Received: May 2, 2013
Revised: June 21, 2013
Published online on September 12, 2013

© 2013 Wiley-VCH Verlag GmbH & Co. KGaA, Weinheim